Available online at www.sciencedirect.com
ScienceDirect
Polymer 49 (2008) 1338–1349
polymer
www.elsevier.com/locate/polymer

Anisotropic actuation of mechanically textured polypyrrole films

Rachel Z. Pytel [a,1], Edwin L. Thomas [a,*], Yi Chen [b,2], Ian W. Hunter [b,2]

[a] *Department of Materials Science and Engineering, Massachusetts Institute of Technology, 6-113, 77 Massachusetts Avenue, Cambridge, MA 02139, United States*

[b] *Department of Mechanical Engineering, Massachusetts Institute of Technology, 3-154, 77 Massachusetts Avenue, Cambridge, MA 02139, United States*

Received 25 September 2007; received in revised form 24 December 2007; accepted 5 January 2008
Available online 11 January 2008

Abstract

Free-standing polypyrrole films have been stretched or cold rolled to produce uniaxially and biaxially textured films. The oriented films show an increase in conductivity up to 3× when compared to unprocessed films, due to polymer chain alignment. Highly anisotropic active stress and strain are observed for the textured films, with up to 7× larger active strains *transverse* to the orientation direction. This anisotropy results in a 100% increase in active stress and 70% increase in active strain when compared to unprocessed films, and active strains over 10% (when cycled at 0.1 V/s) have been achieved with this method.

Keywords: Polypyrrole; Actuator; Microstructure

1. Introduction

Polypyrrole is an interesting conducting polymer for development as an actuator material, due to the high power density and active stresses achievable as well as the fact that the material can be actuated at very low voltages (0.5–3 V). We electrodeposited free-standing polypyrrole films and then manipulated the structure of those films via post-synthesis processing. By manipulating the nanoscale chain configuration and packing, we exploited the connection between nanoscale transport events and macroscale active strain to make better conducting polymer electroactive devices. Previous groups have utilized synthetic variables to impart an anisotropic structure to very small (10^{-6} mm^2) polypyrrole samples on a rigid substrate [1,2]. Here we take free-standing polypyrrole films produced on a much larger scale (14,000 mm^2) and process them by post-synthesis to obtain free-standing anisotropic actuators.

Stretched conducting polymer films have previously been shown to have anisotropic conductivity [3–5] and in polyaniline, anisotropic electroactive strain [6]. Our group has recently employed post-deposition deformation processing to improve electroactive properties of polypyrrole films doped with hexafluorophosphate [7]. In the present study we further probe the uniaxial texture imparted by stretching as well as use cold rolling to impart a biaxial texture to polypyrrole films. We had hoped that the additional organization present in the biaxial microstructure would produce ordered channels in which ions could easily travel through the film, improving the electroactive properties even beyond what is achievable in uniaxially drawn films. Wide-angle X-ray diffraction was used to evaluate the microstructure of the stretched and rolled films, and showed significant polymer chain orientation without an appreciable change in the 2θ breadth of the diffraction peaks. This chain orientation led to anisotropy in conductivity, elastic modulus, and electroactive response for both the stretched and rolled films. The anisotropy of electroactive response was dependent on the rate of electrochemical actuation, and we discuss the deformation of interchain spaces during processing that could be responsible for the anisotropy and the time dependence of the electroactive response.

* Corresponding author. Tel.: +1 617 253 5931; fax: +1 617 252 1175.
E-mail addresses: elt@mit.edu (E.L. Thomas), ihunter@mit.edu (I.W. Hunter).
[1] Tel.: +1 617 253 5931; fax: +1 617 252 1175.
[2] Tel.: +1 617 253 3921; fax: +1 617 252 1849.

0032-3861/$ - see front matter © 2008 Elsevier Ltd. All rights reserved.
doi:10.1016/j.polymer.2008.01.006

2. Experimental

2.1. Polypyrrole film synthesis

Polypyrrole films were deposited electrochemically onto a glassy carbon electrode and then peeled off the electrode for processing and testing. The solution used for most films consisted of 0.05 M tetrabutylammonium hexafluorophosphate (TBAPF6), 0.05 M pyrrole and 1 vol% water in propylene carbonate. The deposition was carried out at a constant current density of 1 A/m^2, at a temperature of −40 °C, with a copper foil counter electrode. These deposition conditions will be referred to as ''TBAPF6/PC'' and are the conditions used when not otherwise specified. For comparison, additional samples were deposited from 0.2 M pyrrole, 0.2 M lithium bis(trifluoromethanesulfonyl)imide in methyl benzoate (LiTFSI/MB) [8] or 0.2 M pyrrole, and 0.2 M TBAPF6 in methyl benzoate (TBAPF6/MB). Pyrrole (Aldrich 99%) was vacuum distilled before use. All other materials were used as-received.

2.2. Polypyrrole film processing

After synthesis, large area films (70 mm × 230 mm × 0.03 mm) were peeled off from the working electrode and stored in ambient conditions. Sections of these films (50 mm × 150 mm) were stretched up to 100% linear elongation by a Zwick/Roell Z010 Mechanical Tester under stress control, at a rate of 0.0167 MPa/min. The stretched film specimens will be referred to as ''S''. Different sections (20 mm × 60 mm) of the as-deposited films were mechanically rolled up to 70% linear elongation using a Durston C130 rolling mill. The rolled film specimens will be referred to as ''R''. All films were processed at room temperature, in air, within two days of deposition. The coordinate system used for oriented samples is defined as

- ND (normal direction) = normal to the surface of the film
- MD (machine direction) = parallel to the stretch or roll direction
- TD (transverse direction) = perpendicular to the MD and ND

Samples for electroactive testing (2 mm × 15 mm) were cut from the stretched and rolled films, some with their long axis parallel to the machine direction (labeled S_{MD} and R_{MD}) and some with their long axis perpendicular to the machine direction (labeled S_{TD} and R_{TD}). For comparison, 2 mm × 15 mm samples were cut from the as-deposited polypyrrole film with no additional processing (labeled ''A'').

2.3. Polypyrrole film testing

After processing, films were stored at ambient conditions. The conductivity of each sample was measured using a standard four-point probe. Wide-angle X-ray diffraction patterns were taken under vacuum, using Fuji BAS-MS image plates. Single polypyrrole films were exposed with the incident X-ray beam (q_o) parallel to the ND. For q_o parallel to the MD or TD, small strips of polypyrrole (approximately 1 mm × 3 mm) were cut from larger samples in the MD or TD with care to maintain orientation, and stacked to a thickness of approximately 0.75 mm for exposure to the X-ray beam. The diffraction patterns were integrated using the Polar software package, developed at Brookhaven National Laboratories [9].

Mechanical properties and electroactive properties were measured on a custom-built dynamic mechanical analyzer within one week of deposition and processing [10]. This apparatus allows one to clamp the polypyrrole film under tension in a three-electrode electrochemical cell and measure the electroactive response that occurs upon application of a potential waveform. For our experiments, a stainless steel counter electrode and silver wire reference electrode were used. The electrolyte was neat 1-butyl-3-methylimadazolium hexafluorophosphate (BMIMPF6). Before submersion in the electrolyte, the passive elastic modulus of each sample was measured by application of a 1% strain at a frequency of 1 Hz. After the initial modulus measurement, the film was slackened, submersed into electrolyte, and ''warmed up'' by application of a ±2 V triangle wave at 0.1 V/s until the current response stabilized.

After warm-up, the films were measured in both isotonic and isometric modes. In isotonic mode, the films were held at a constant load (0.5 MPa) in the electrolyte. A potential waveform was applied and the resulting length change was measured. The ''active strain'' is the contractile strain observed. In isometric mode, the film was held under tension at a constant length (approximately 1% strain). A potential waveform was applied and the change in stress was measured. The ''active stress'' is the magnitude of the stress response.

3. Results

3.1. Wide-angle X-ray diffraction

Uniaxial stretching causes the polypyrrole chain axes to align in the MD, leading to anisotropic scattering visible via X-ray diffraction. Several authors have conducted X-ray diffraction on stretched polypyrrole films to differentiate between characteristic reflections that occur parallel and perpendicular to the chain axis and assign these reflections to physical features [4,5,11,12]. A schematic of these characteristic reflections is shown in Fig. 1(1) and a diffraction pattern from a film stretched as part of this work is shown in Fig. 1(2). We use the letters ''**a**–**c**, **Γ**'' to describe the characteristic reflections in polypyrrole. While this notation suggests a crystalline unit cell, diffraction patterns of polypyrrole show that the films do not contain large amounts of crystalline material, as will be discussed shortly. Instead, there are very small well-ordered regions (''chain bundles'') within a relatively disordered matrix, as is shown schematically in Fig. 3(3) and expanded upon in Section 4.

Reflection **a** occurs at 3.4 Å and is attributed to the face-to-face distance between polypyrrole rings on adjacent stacked planar chains [4,7,11,13–15]. This assignment is shown in Fig. 3(2) and is supported by the fact that in oriented films,

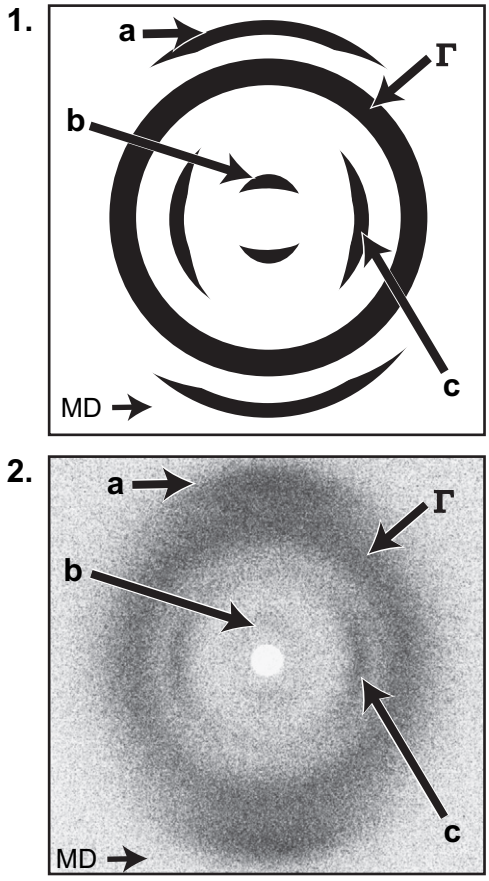

Fig. 1. Diagram of characteristic reflections in polypyrrole. (1) Schematic of characteristic reflections observed in wide-angle X-ray diffraction patterns of stretched films. Machine direction is horizontal. (2) Example of wide-angle X-ray diffraction pattern from stretched film. The MD is horizontal.

this spacing occurs perpendicular to the chain axis. Reflection **b** is observed at *d* spacings of 13–22 Å and also orients perpendicular to the chain axis. This reflection has been observed to increase to a larger *d* spacing as larger counterions are used in deposition [5,16], suggesting that it corresponds to the distance between stacks of polypyrrole chains separated by counterions. When larger counterions sit between the stacks of polypyrrole chains, the stacks move further apart causing the *d* spacing of reflection **b** to increase. Reflection **c** orients parallel to the chain axis and has been attributed to a feature repeated along the polymer chain. Yamaura et al. observed this reflection at 7.3 Å and assigned it to the trans-planar dipyrrole repeat [5]. Nogami et al. observed reflection **c** at a spacing at 6.46 Å and attributed the difference from the measured size of a dipyrrole unit to the polypyrrole chains having an axial tilting of 25–30° from the machine direction [11]. However, it is expected that the chain axes will align in the MD upon stretching, and we find no logical reason for the chain axes to assume a regular 25° deviation from the MD. Furthermore, a tilting of the chain axes should also cause a deviation in reflection **a**, which neither we nor Nogami et al. observe [11]. It is possible that the deviation of the spacing corresponding to reflection **c** from the size of the dipyrrole unit is caused by a staggering of polypyrrole chains that are axially aligned in the MD, as was also proposed by Nogami et al. (though they do not discuss its implications for *d* spacing of reflection **c** [11]) and is schematically illustrated in Fig. 2. Similarly to what has been previously observed in polyurethanes [17–19], the arrangement shown in Fig. 2 would result in two diffraction maxima approximately ±28° from the MD at 6.6 Å instead of one peak along the MD at 7.3 Å. We observe reflection **c** at approximately 6.6 Å and while we do not observe two separate maxima, the peak is so azimuthally broad that the two maxima could be overlapped. While the reason for the observed deviation from the dipyrrole spacing cannot be conclusively determined due to the ambiguous diffraction pattern, we believe it more likely to be caused by a regular offset of the polypyrrole chains than a regular tilting of the chain axes away from the MD.

Reflection **Γ** does not become anisotropic upon stretch and has previously been attributed to scattering from the amorphous polymer chains [11,15,20]. This assignment implies there is no substantial contribution from PF_6^- scattering to diffraction pattern, which is highly unlikely given the fact that the PF_6^- anions contain the highest atomic number elements in the system. Furthermore, even non-crystalline polymer chains will assume axial orientation in the MD (leading to anisotropic X-ray scattering) upon stretching below their T_g. Polypyrrole doped with *p*-toluene sulfonate has been shown to have a T_g of about ~50 °C when polymerized from propylene carbonate [21] and a T_g of about ~150 °C when polymerized from aqueous solution [22], and T_g may also change depending on the redox state of the polymer. We have not observed a clear T_g

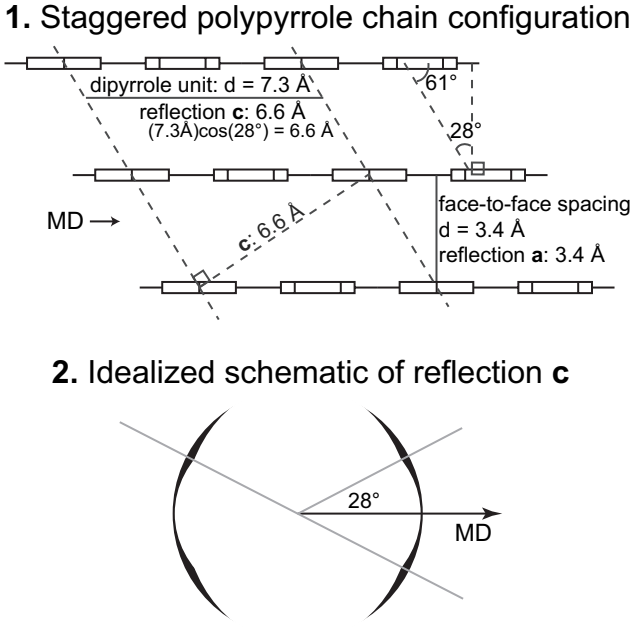

Fig. 2. (1) Schematic illustration of proposed staggered polypyrrole chain model. The polypyrrole chain axes align in the MD (horizontal), but are offset from each other along the chain axis causing reflection **c** to be observed at 6.6 Å instead of at the dipyrrole repeat spacing of 7.3 Å. (2) Schematic of intensity distribution from the characteristic reflection **c** that would result from the staggered model shown in (1) along with finite misorientation of the chain axis along the MD.

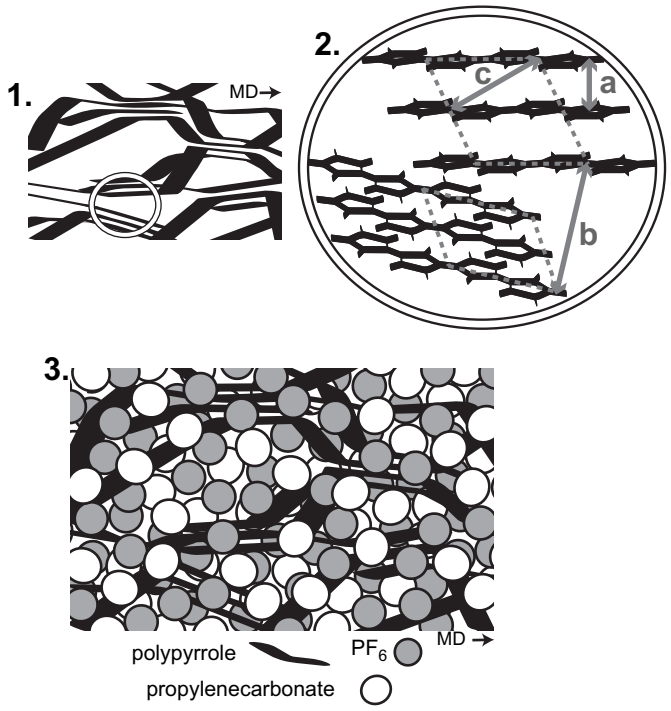

Fig. 3. (1) Diagram of polypyrrole film held together by small well-ordered polymer regions, which we refer to as ''chain bundles''. The chain axes and bundles are oriented in the MD. (2) Magnified diagram of two chain bundles from (1), with the physical origins of characteristic reflections **a**–**c** identified. (3) Diagram of components of stretched polypyrrole film. The chain axes and bundles are preferentially oriented in the MD, while the PF_6^- anions and propylene carbonate are randomly distributed throughout the non-bundled regions. Note the large volume fraction (~60%) of non-polymeric molecules in the film.

in our polypyrrole films, but based on the published results for other polypyrrole systems and the stiff nature of the films we produce, T_g for our films is well above room temperature. Therefore, instead of arising from scattering from amorphous polymer chains, reflection **Γ** must be primarily due to correlations between small molecules that do not assume preferential orientation upon stretching. It has previously been reported to be caused by solvent [23] or counterion [5,14,24] scattering.

By changing the solvent and counterion used for deposition, we can investigate how reflection **Γ** depends on the scattering from the small molecules in the system. Thus, when the solvent is changed from propylene carbonate to methyl benzoate, the position of reflection **Γ** remains the same (Fig. 4). When the counterion is changed to a larger species, the d spacing corresponding to reflection **Γ** increases (q_{peak} shifts from $q = 1.4$ Å^{-1} to $q = 1.26$ Å^{-1}). Unlike previous studies [5,16], in our work, there is not a clear trend in the position of reflection **b** when the counterion is changed, as the position of reflection **b** also seems to be sensitive to the solvent and electrode material.

X-ray diffraction measurements were taken from as-deposited, stretched and rolled films with the incident X-ray beam (q_o) parallel to all three axes. The 2D diffraction pattern for an as-deposited polypyrrole film is shown in Fig. 5. For the as-deposited film, characteristic reflections **a**–**c** and **Γ** do not show anisotropy in any direction. As expected, the

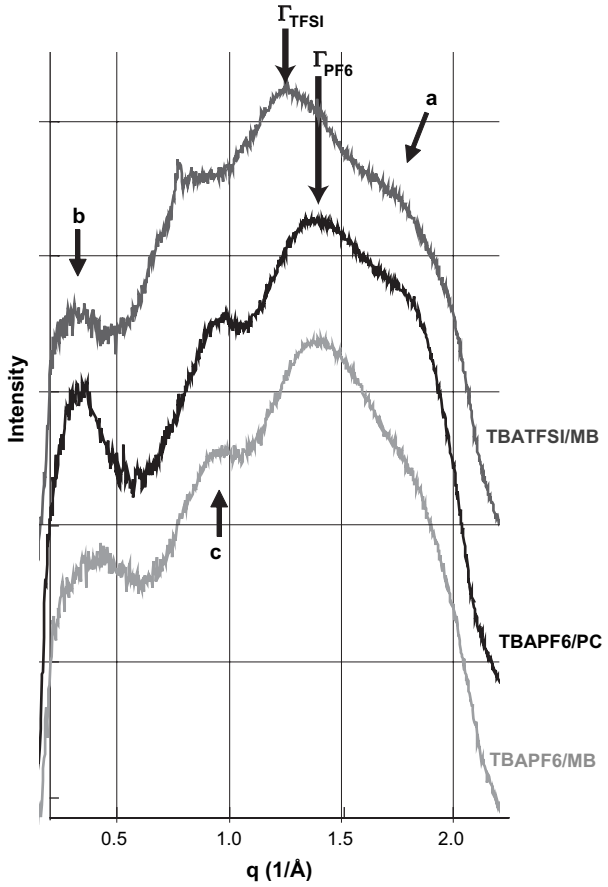

Fig. 4. Wide-angle X-ray scattering from films prepared from different deposition solutions. Curves are vertically offset for clarity. Reflection **Γ** occurs at $q = 1.4$ Å^{-1} for TBAPF6/PC and TBAPF6/MB, and at $q = 1.26$ Å^{-1} for TBATFSI/MB. This corresponds to the larger size of the $TFSI^-$ anion ($r = 3.25$ Å) [25] when compared to the PF_6^- anion ($r = 2.54$ Å) [25]. The sharp peak in the TBATFSI/MB curve at $q = 0.77$ Å^{-1} is due to contamination.

polypyrrole chains are randomly oriented throughout the as-deposited sample. When q_o is parallel to the ND and MD the diffraction patterns have identical features to the one shown, showing that the as-deposited film is isotropic.

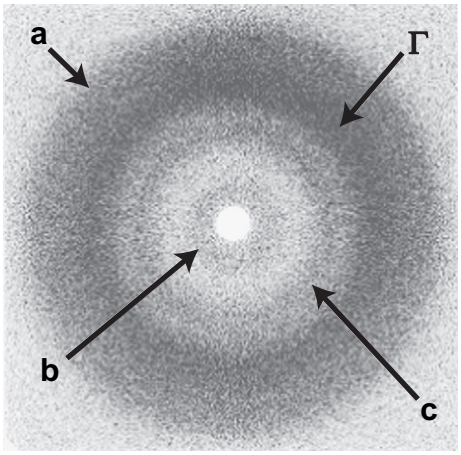

Fig. 5. Wide-angle X-ray scattering of unprocessed polypyrrole with q_o parallel to the ND. Reflections **a**–**c** and **Γ** all appear as isotropic rings, due to the lack of preferential orientation.

Wide-angle X-ray patterns for stretched and rolled polypyrrole are shown in Figs. 6–8. For the stretched films, reflection **c** (which arises from correlations along the chain axis) clearly aligns in the MD (Fig. 8(1)). Reflections **a** and **b** occur transverse to the chain axis, so they are absent in the MD and instead they appear in the ND and TD as is expected for uniaxial alignment along the MD. As one increases the elongation of the stretched films, the orientation improves and less scattering from reflection **c** is visible in the ND and TD. However, because these peaks are poorly defined and overlapping, we were not able to quantitatively calculate Herman's orientation parameters.

In the rolled films, reflection **c** again appears most strongly along the MD, confirming axial chain alignment with the MD (as shown in Fig. 8(2)). However, in this case reflection **a** appears in the ND and not in the TD (so it is visible in Fig. 7(2) but not in Fig. 7(1)), while reflection **b** appears in the TD and not in the ND (so it is visible in Fig. 7(1) but not in Fig. 7(2)). This shows that rolling aligns the chain axes in the MD, but the chains assume an additional degree of orientation with the polypyrrole rings parallel to the surface of the film. This is the first time that this biaxial texture has been shown in polypyrrole, where reflections **a** and **b** appear perpendicular to each other.

3.2. Effect of processing on electroactive response

Fig. 9 compares the electroactive strain response for stretched and for rolled films to that of an unprocessed film. For the conditions shown in Fig. 9, the as-deposited film shows an active strain of $\varepsilon_A = 4.7\%$. The rolled film shows an active strain of $\varepsilon_{MD} = 1.5\%$ in the MD and $\varepsilon_{TD} = 8.9\%$ in the TD. The stretched film shows an active strain of $\varepsilon_{MD} = 1.4\%$ in the MD and $\varepsilon_{TD} = 9.6\%$ in the TD. The as-deposited and TD films (for both stretched and rolled samples) show an overall greater extension than contraction, as will be discussed later.

Both the stretched and rolled samples tested shown in Fig. 9 were cut from films processed to approximately 55% linear elongation. However, not every point in the processed film has the same degree of polymer chain orientation due to localized plastic deformation. We use the local conductivity and local elastic modulus to compare the degree of orientation in small samples. In a perfectly oriented conducting polymer

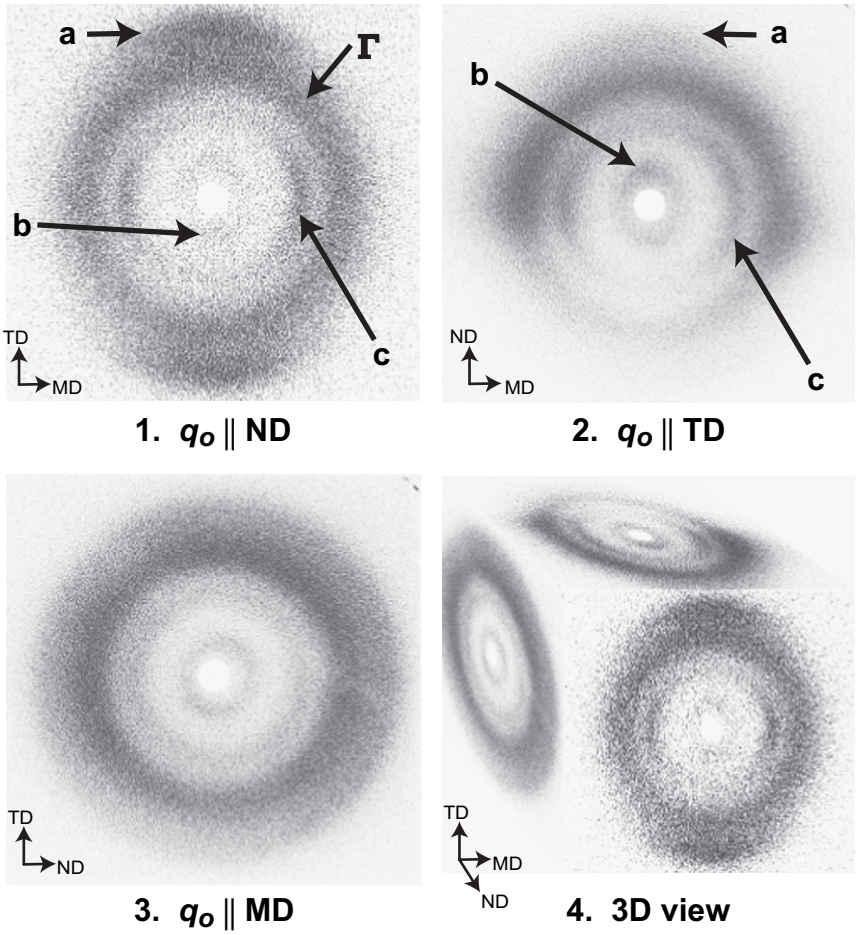

Fig. 6. Wide-angle X-ray scattering of stretched polypyrrole. Reflections **a** and **b** orient in the ND and TD, while reflection **c** orients in the MD as seen in (1) and (2). The diffraction pattern when $q_o \parallel$ MD is isotropic as seen in (3), confirming uniaxial alignment in the MD. Reflection **Γ** does not orient and remains an isotropic ring in all viewing directions. Some shadowing from the clamps holding the films in the X-ray beam is visible in the $q_o \parallel$ TD image (2).

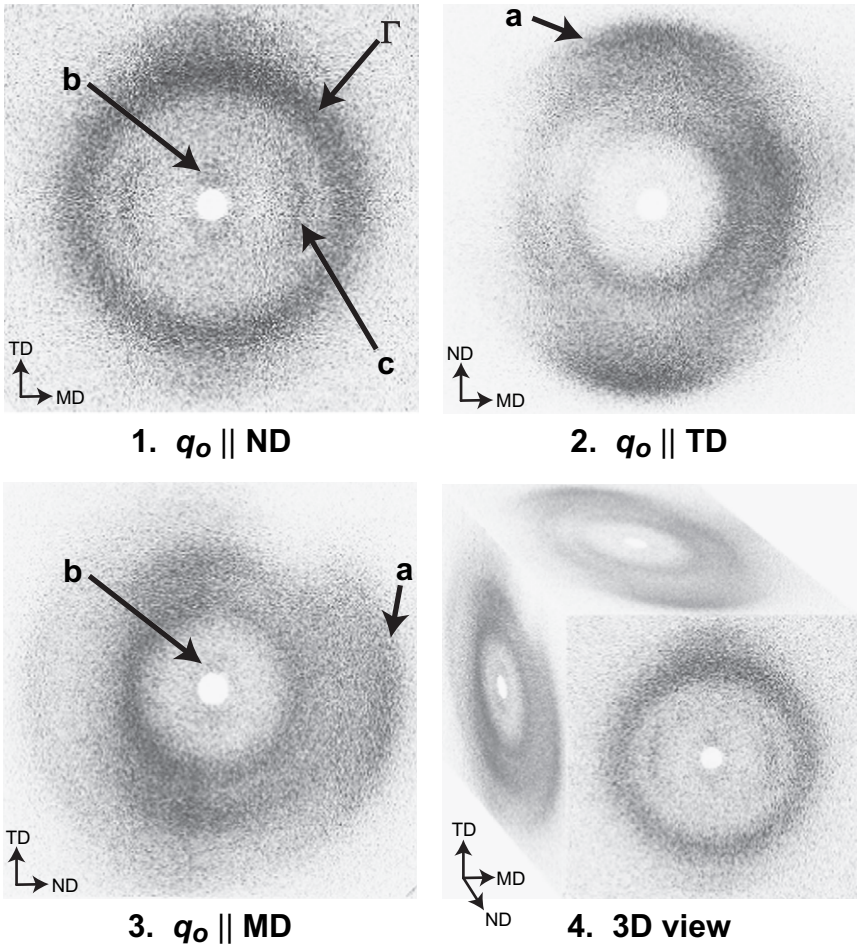

Fig. 7. Wide-angle X-ray scattering of rolled polypyrrole. Reflection **a** orients in the ND, so it is barely visible in the q_o || ND pattern (1). Reflection **b** orients in the TD, so it is not observed in the q_o || ND pattern (2). Reflection **c** primarily orients in the MD. Reflection **Γ** does not orient. Some clamp shadowing is visible on the q_o || TD and q_o || MD images (2 and 3).

film, the polymer chains will be axially aligned with the MD. For such a sample, one would observe a very high conductivity and elastic modulus in the MD because the measurement captures the high conductivity and modulus of the polymer backbone, and a much lower conductivity and elastic modulus in the TD because of the lower interchain conductivity and relatively weak interchain bonding. Therefore, a larger anisotropy in conductivity (σ_{MD}/σ_{TD}) and elastic modulus (E_{MD}/E_{TD}) is indicative of a larger degree of axial orientation in the MD. As shown in Table 1, on this basis the rolled samples show slightly better orientation than the stretched samples. However, the stretched samples show a larger electroactive effect for isotonic testing. Similar results are observed for isometric testing, an example of which is shown in Fig. 10.

Changing the voltage ramp, we observe a difference in the amount of active strain observed and the amount of irrecoverable length change. As shown in Fig. 11, when stretched films are actuated at 0.1 V/s, an active strain of 11.3% is observed in the TD. As the voltage ramp is increased, the time for each cycle decreases, as does the magnitude and anisotropy of active strain. When the films in Fig. 11 are cycled at 0.1 V/s, $(\varepsilon_{TD}/\varepsilon_{MD})_S = 6.2$. When the voltage ramp is increased to 1 V/s, the anisotropy of active strain decreases with $(\varepsilon_{TD}/\varepsilon_{MD})_S = 3.8$.

4. Discussion

4.1. Polypyrrole microstructure

The diffraction patterns shown in Figs. 2–6 contain broad, overlapping peaks that cannot be quantitatively separated, even in highly processed films. The ambiguous shapes of the individual peaks prevent accurate calculation of the average crystallite size via the Scherrer equation [26,27]. Estimates of crystal size using this method result in crystallites of 10–20 Å in diameter, which contain only up to five repeat units for reflection **a** and two repeat units for reflection **c**. If the size of the ordered regions in polypyrrole is not larger than a few stacked chains, the label of "crystal" is somewhat tenuous. The microstructure is best visualized as containing small "bundles" of polypyrrole chains stacked over a few repeat units (two bundles with three repeat units for reflection **a** and two repeat units for reflection **c** are highlighted in Fig. 3(2)). These very small bundles of polypyrrole chains

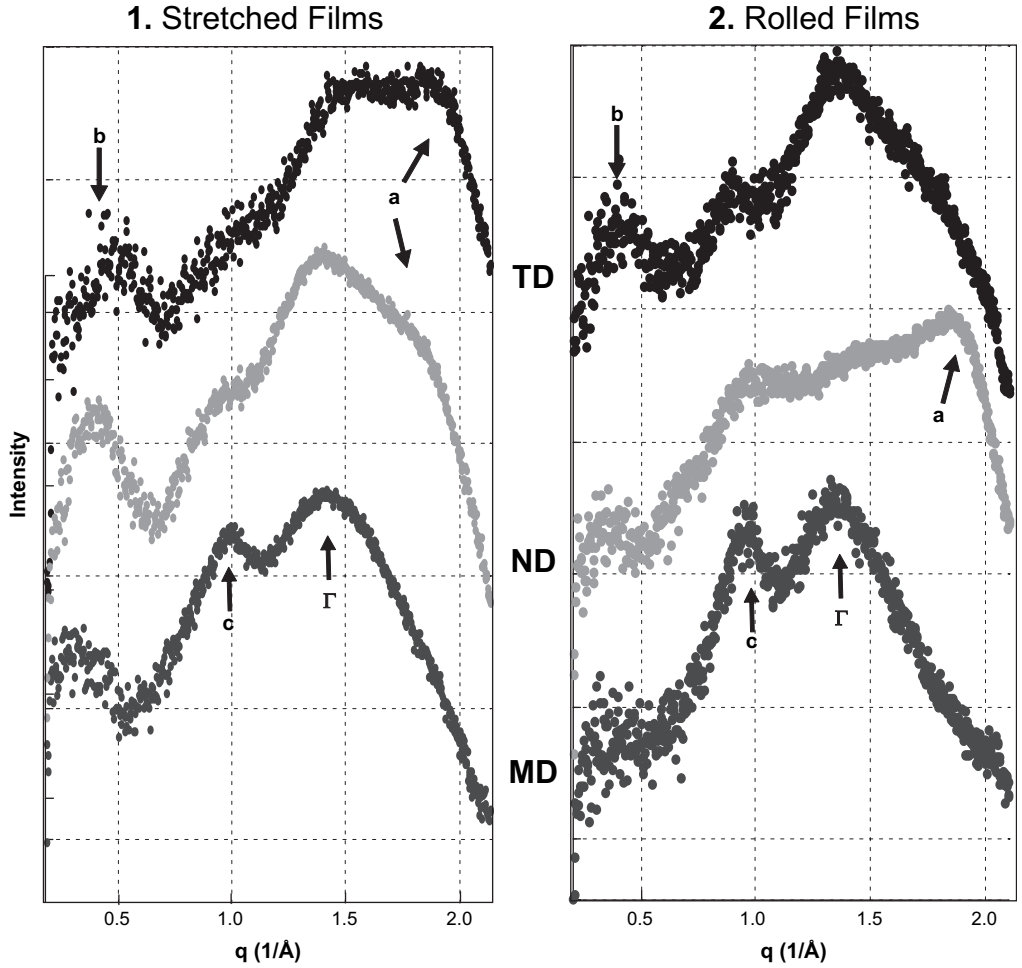

Fig. 8. 1D views of WAXS patterns for stretched and rolled films, vertically offset for clarity. The 1D patterns were obtained by integrating the 2D patterns shown in Figs. 6 and 7 over the range ±10° around the direction of interest. For example, the "TD" curve in Fig. 8(1) was obtained by integrating Fig. 6(1) from −10° to 10° (where 0 is vertically up from center). (1) Stretched films. Reflections **a** and **b** can be observed in the TD and ND. Reflection **c** is most clear in the machine direction, but some scattering from reflection **c** is evident in the other two directions. Reflection **Γ** does not clearly orient in any direction, as it is observed in all three curves. (2) Rolled films. Reflection **a** is most clear in the normal direction. Reflection **b** is most clear in the transverse direction. Reflection **c** is most clear in the machine direction, but some scattering from reflection **c** is evident in the other two directions. Reflection **Γ** does not clearly orient in any direction, but is more easily observed in the TD and MD than in the ND. This may be because it is overlapping with reflection **a** in the ND.

provide the characteristic reflections observed in the diffraction patterns, but their small size causes the peaks to be broad and overlapping, preventing a full crystallographic characterization of the material. These bundles become oriented with processing, as the polypyrrole chain axes align in the MD. The fact that the counterions (observed via reflection **Γ**) do not become oriented with processing shows that the counterions are not part of these bundles, and are instead isotropically distributed throughout the film, around and in between the bundles.

Determination of percent crystallinity from X-ray diffraction patterns requires the separation of crystalline peaks from broad amorphous halo(s). In polypyrrole the different peaks cannot be clearly separated, and there is no discernable difference in shape between peaks that have previously been assigned to "crystalline" scattering or "amorphous" scattering. Even if one assigns reflection **Γ** to non-crystalline PF_6^- anions, the broad, overlapping nature of the other reflections prevents one from unambiguously separating them from an "amorphous" contribution to quantify the percent crystallinity based on the diffraction pattern. The assignment of a Gaussian fit of reflection **Γ** to the non-crystalline component in the sample has previously led to incorrect estimates of percent crystallinity, up to 50% for polypyrrole doped with PF_6^- [15,20]. This is an extremely high value considering the lack of clear crystalline peaks in the diffraction pattern, and a typical doping level of one PF_6^- anion for every three pyrrole rings in the as-deposited film (so at least 30 vol% of the film is non-crystalline PF_6^-).

Even though they are not a majority component of the material, the chain bundles have a significant effect on polypyrrole's mechanical and electrical properties. We suggest the bundled chain segments are tightly held together due to π-orbital overlap. The bundles act as physical cross-links, connecting the chains within the polypyrrole matrix as shown in Fig. 3(1). Elemental analysis of fresh polypyrrole films deposited from our standard recipe has shown that these films are only approximately 40 wt% polymer, the remainder of the

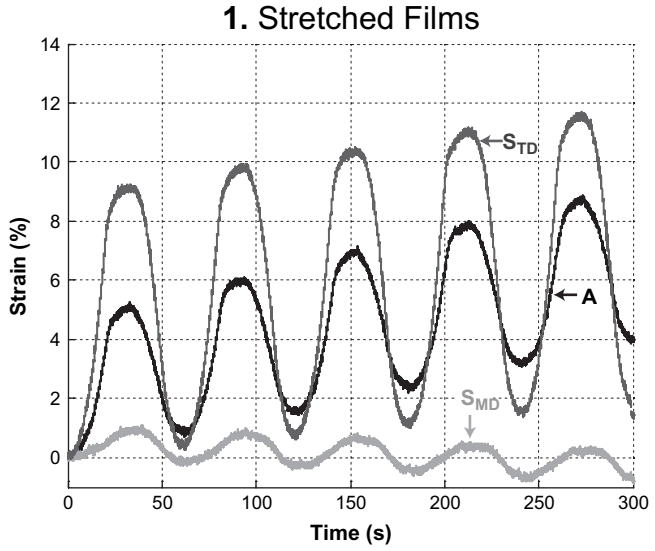

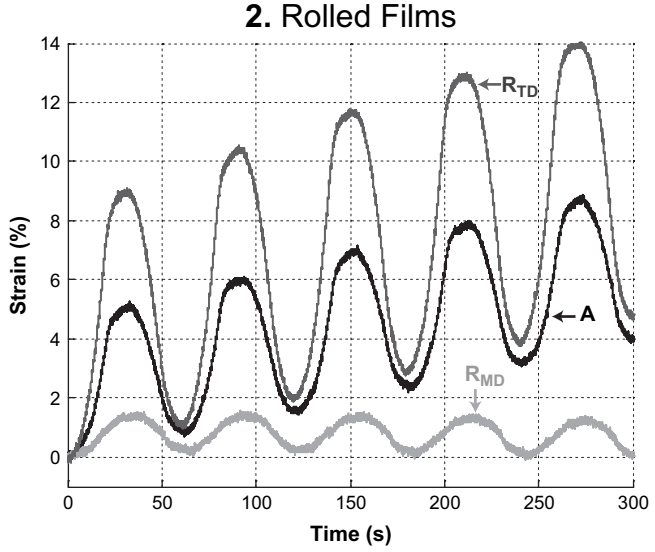

Fig. 9. Isotonic response for stretched and rolled films. Films were held under a static force of 0.5 MPa in neat BMIMPF6 and a ±1.5 V triangle wave in potential was applied at a rate of 0.1 V/s. Strains are normalized by subtracting the initial strain that occurs upon application of the testing load. (1) Films stretched to 55% elongation. Under these conditions, $(\varepsilon_{TD}/\varepsilon_{MD})_S = 7.0$. (2) Films rolled to 55% elongation. Under these conditions, $(\varepsilon_{TD}/\varepsilon_{MD})_R = 5.9$.

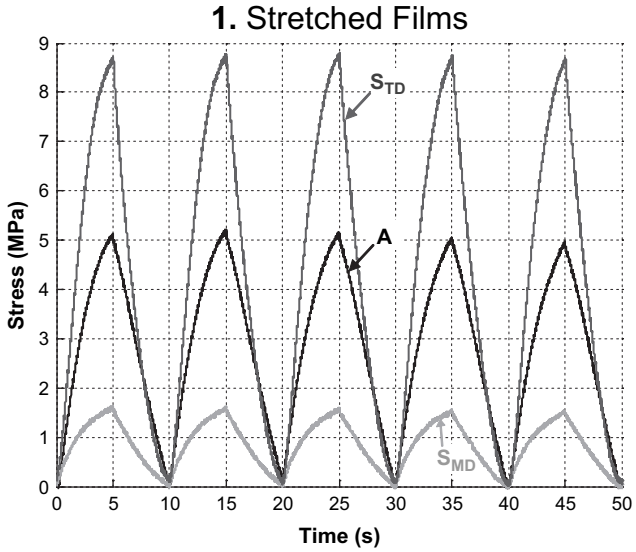

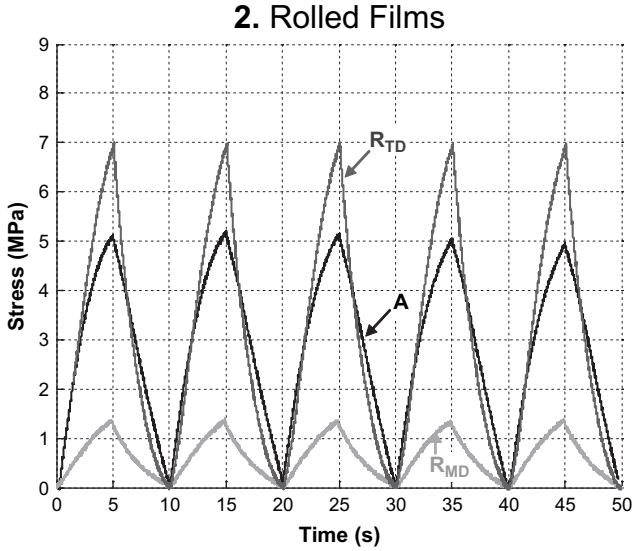

Fig. 10. Isometric actuation of stretched and rolled films. Films were held under a static strain of 1% in neat BMIMPF6 and a ±1.5 V square wave was applied at a frequency of 0.1 Hz. Stresses are normalized by subtracting the stress at time = 0 s. (1) Films stretched to 55% elongation. Under these conditions, $(\text{stress}_{TD}/\text{stress}_{MD})_S = 5.4$. (2) Films rolled to 55% elongation. Under these conditions, $(\text{stress}_{TD}/\text{stress}_{MD})_R = 5.0$.

Table 1
Electroactive results for as-processed, stretched and rolled films, tested in neat BMIMPF6

Treatment	Direction	σ (10^4 S/m)	σ_{MD}/σ_{TD}	E (GPa)	E_{MD}/E_{TD}	ε[a] (%)	$\varepsilon_{MD}/\varepsilon_{TD}$	Stress[b] (MPa)	$\text{Stress}_{MD}/\text{stress}_{TD}$[b]
None		2.4		0.4		4.7		5.2	
Roll ~ 55%	MD	5.3	4.7	0.5	1.5	1.5		1.4	
	TD	1.1		0.3		8.9	5.9	7.0	4.9
Stretch ~ 55%	MD	5.0	3.8	0.4	1.4	1.4		1.6	
	TD	1.3		0.3		9.6	7.0	8.8	5.4

Conductivity (σ) and elastic modulus (E) are measured as described in Section 2.

[a] Isotonic testing under conditions shown in Fig. 9.

[b] Isometric testing under conditions shown in Fig. 10.

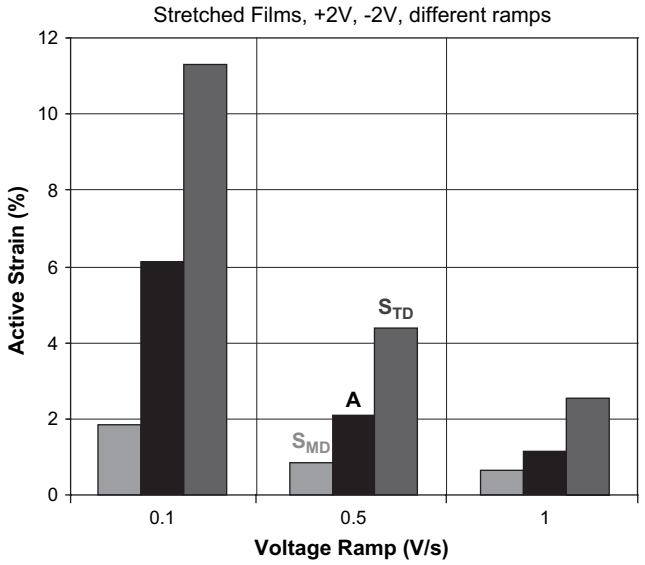

Fig. 11. Isotonic testing of stretched samples in neat BMIMPF6 with a static force of 0.5 MPa. A ±2 V potential triangle wave was applied with the voltage ramp indicated. Strains are normalized by subtracting the initial strain that occurs upon application of the static force. Light grey bars: S_{MD}. Black bars: A. Dark grey bars: S_{TD}. At 0.1 V/s, $(\varepsilon_{TD}/\varepsilon_{MD})_S = 6.2$. At 0.5 V/s, $(\varepsilon_{TD}/\varepsilon_{MD})_S = 5.3$. At 1 V/s, $(\varepsilon_{TD}/\varepsilon_{MD})_S = 3.8$.

film consisting of approximately equal parts of PF_6^- and propylene carbonate. The bundles allow the polypyrrole chains to form a percolative path that dominates the films' mechanical properties, resulting in a robust film even though a majority of the total film material consists of small molecules that cannot support a tensile load. Polypyrrole bundles are illustrated with the other components in the film in Fig. 3(3). The bundled network provides the high electronic conductivity (2.4×10^4 S/m) and high elastic modulus (0.4 GPa) of the as-deposited film, because the network consists of individual and bundled highly conductive and rigid chains. Furthermore, the bundle regions improve interchain charge transfer via π-overlap beyond what would be achievable in a polymer that was only physically entangled.

4.2. Textures in processed films

While both the stretched and rolled films show polymer chain alignment in the MD, the X-ray diffraction patterns show that the 3D distributions of the polypyrrole chains (and bundles) are different. The polypyrrole chain orientations for as-deposited, stretched, and rolled films are schematically illustrated in Fig. 12. Note that Fig. 12 is intended to clearly show the preferential orientation of the small polypyrrole bundles, not accurately describing the level of disorder of all components in this system. The stretched films show alignment in only one direction, with the chain axes parallel to the MD.

The rolled films show a double texture, with the chain axes parallel to the MD and the aromatic ring normals parallel to the ND. However, the degree of orientation in the MD and ND is not necessarily the same. In the rolled films (Fig. 8(2)) reflection **a** is highly anisotropic, observed only in the ND. This means that the pyrrole ring normals are very well oriented in the ND. Conversely, while reflection **c** is most intense in the MD, some scattering from reflection **c** is observed in all directions. This means that while the chain axes are preferentially oriented in the MD, they are not as well oriented as the pyrrole ring normals (as shown in Fig. 12(3)). While we do not measure the forces applied during our rolling process, these results suggest that the rollers exert enough compressive stress to force the planar chains to lie in the MD/TD plane but not enough tensile deformation to perfectly align the chain axes in the MD. Furthermore, tilting of the chains such that the ring normal is in the ND may be considerably easier than organizing the chains such that they are parallel to the MD, as it would not require the same extent of disentanglement and rearrangement. A given chain segment or bundle could rotate to line up its pyrrole ring normals to the ND without requiring significant cooperativity amongst the units.

The stretched films show a larger electroactive response than do the rolled films, even in cases where the rolled samples show a slightly more anisotropic conductivity and elastic modulus (as for the films in Table 1). This may be because of the

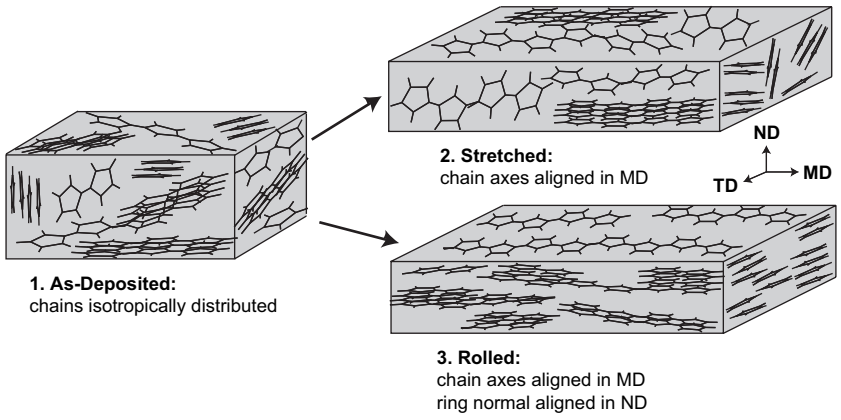

Fig. 12. Microstructure of polypyrrole chains in as-deposited and processed films. (1) As-deposited, unprocessed film. The polypyrrole chains (in both bundled and disordered regions) are isotropically distributed. (2) Stretched film. Bundled and non-bundled polypyrrole chains are axially oriented in the MD, and randomly distributed and tilted around the MD (uniaxial orientation). (3) Rolled film. Bundled and non-bundled chains are axially oriented in the MD, and the pyrrole ring normals are preferentially oriented in the ND (biaxial orientation).

additional degree of orientation present in the rolled films when compared to the stretched films. In the rolled films the pyrrole ring normals are parallel to the ND, but the chains still have a large distribution of orientation about the MD. This distribution of planar chains with their faces parallel to the film surface may impede ion diffusion from the surface of the film.

4.3. Anisotropic actuation

Reduction of polypyrrole in neat BMIMPF6 leads to lateral film expansion as cations swell the film. These cations must find space between polymer chains, so the active strain occurs perpendicular to the chain axis. In unprocessed films, the chain axes are randomly distributed, so swelling and deswelling are observed equally in all directions. In oriented films (both stretched and rolled) the chain axis direction is preferentially aligned with the MD, so the observed active strain is concentrated perpendicular to the MD as shown in Fig. 14. The small amount of active strain observed in the MD is likely due to the swelling of the misoriented chain component. Molecular modeling has suggested that there may be an intrinsic actuation mechanism that would produce a 30% strain along the chain axis for isolated polypyrrole chains, as the chain straightens and curls upon oxidation and reduction [28]. Our results show that this is not a dominant mechanism in polypyrrole films.

With the methodology described in Section 2, we are limited to measuring the electroactive response in the MD and TD. Therefore, it is yet unclear whether the response in the ND is larger for stretched or rolled films. Stretched films should show an equal electroactive response in the ND and TD due to their uniaxial orientation, while the rolled films may show a very different response because the polypyrrole chain orientations in the ND and TD are different. In order to investigate this matter, instrumentation is currently being developed to measure the electroactive response in the ND for a free-standing processed film.

For the data shown in Fig. 9, 30–36 mC of charge was passed during expansion portion of each cycle for each set of films. The passage of a comparable amount of charge implies incorporation of a comparable number of cations, and should result in comparable volumetric expansion. With our testing methodology expansion and contraction are only measured in one direction at a time. When an S_{MD} or R_{MD} sample is actuated, it is likely that the film is expanding and contracting significantly perpendicular to the measured direction. This will be the case for both uniaxially and biaxially oriented films. Future work could include instrumentation to systematically examine actuation in several dimensions at once, as this is where additional differences between actuation in uniaxially and biaxially oriented films will arise. However, if the goal is to produce an efficient linear actuator, expansion and contraction in directions not harnessed by the device are irrelevant. For these applications, an actuator that effectively actuates in only one direction is ideal.

The electroactive tests presented here were intended to expose the influence of molecular orientation on actuation. Thus, the isotonic tests were limited to 5–10 cycles and a load of 0.5 MPa, in an attempt to minimize molecular re-organization due to the load applied during testing. These conditions are sufficient to capture the anisotropy of active strain, but of insufficient duration to obtain a full picture of the maximum number of cycles achievable in oriented films. Polypyrrole actuated in neat BMIMPF6 has been previously shown to be very stable (a decrease of only 0.2% in active strain was observed over 6000 cycles [29,30]) but thus far only unoriented polypyrrole has been tested. We expect oriented polypyrrole to be equally electrochemically robust when actuated in neat BMIMPF6, but it may not be as physically robust. Because the polypyrrole chains are tied together via bundles, perfect, single crystalline orientation is impossible. The orientation that we achieve captures the polymer chains in a non-equilibrium configuration. As the polymer films are electrochemically cycled, movement of the small counterion molecules plasticizes the film and increases the mobility of the chains. The ion movement and changes in film volume during actuation may allow the polymer chains the mobility needed to revert to a more random orientation. For example, an unrecovered contraction is observed in the S_{MD} and R_{MD} samples in Fig. 9. In this case, the small applied load (only 0.5 MPa) is not enough to prevent the re-orientation of polymer chains away from alignment in the MD. The relaxation of polymer chains from axial alignment in the MD causes the aspect ratio of the oriented sample to decrease, as is schematically illustrated in two dimensions in Fig. 13. This change in aspect ratio is observed as an overall elongation in the S_{TD} and R_{TD} samples and an overall contraction in the S_{MD} and R_{MD} samples in Fig. 9. Unrecovered sample deformation is another area that demands measurement in the ND, in order to fully characterize the change in sample shape.

Unrecovered expansion or contraction upon cycling may be avoided by properly constraining the film. In the isometric test

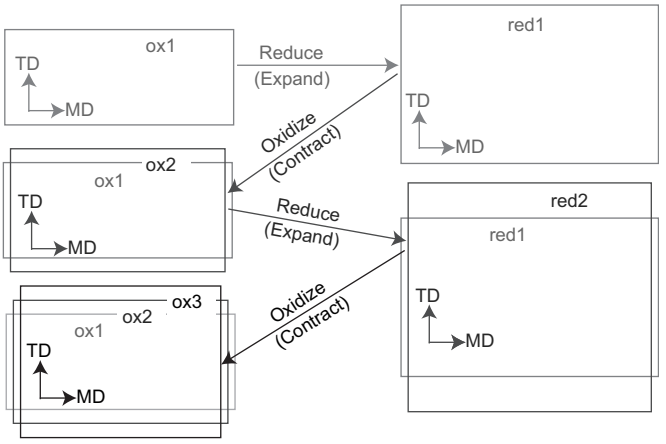

Fig. 13. Schematic (2D) diagram of expansion and contraction for oriented films under conditions shown in Fig. 7. The percentage change in length and width upon oxidation and reduction is exaggerated for clarity. The area of the sample while oxidized is labeled ox1, ox2 and ox3. The area of the sample while reduced is labeled red1 and red2. During each reduction, the area of the sample increases. During each oxidation, the area of the sample decreases. At the end of the redox cycle the sample has relaxed from its original aspect ratio as described in the text.

in Fig. 9, for example, the film is geometrically constrained to maintain a constant length and an irreversible increase or decrease of the active stress is not observed. Furthermore, it may be possible to adjust the electrochemical conditions to find a balance between allowing enough ion movement to cause a large electroactive response and limiting polymer chain mobility to prevent irreversible relaxation. Future work will address the actuation of oriented films over very long times to determine how re-orientation can best be prevented by the design of the loading mechanics and/or applied electrochemistry in electroactive devices.

4.4. Anisotropic diffusivity

When the voltage ramp is increased, the active strain in the TD decreases more than the active strain in the MD, showing that actuation in the TD is more time-limited than in the MD. It has been previously observed that diffusion of small molecules is much higher in the MD than the TD for oriented polycarbonate [31] and other oriented glassy polymers [32]. This has been attributed to a deformation of the free volume in the sample upon polymer orientation, resulting in effective ellipsoids of free volume with their long axis parallel to the MD [31]. In the case of polypyrrole, there are solvent and counterion molecules in the spaces between polymer chains and bundles (so this volume is not entirely ''free'') but these spaces will be elongated with processing as illustrated in Fig. 14. This means that there are effective pathways that allow the small molecules to diffuse more easily along the MD. The lower diffusivity in the TD causes actuation in that direction to be more time-limited than in the MD. Furthermore, as shown in Table 1, the electronic conductivity is significantly lower in the TD than the MD. This will affect the rate of charge injection to the polymer and amplify the difference in actuation speed between samples measured in the TD or MD. If future experiments are conducted using a different geometry (e.g. electrical contacts are made along the MD while strain is measured in the TD) the effects of electronic conductivity and counterion diffusivity may be decoupled.

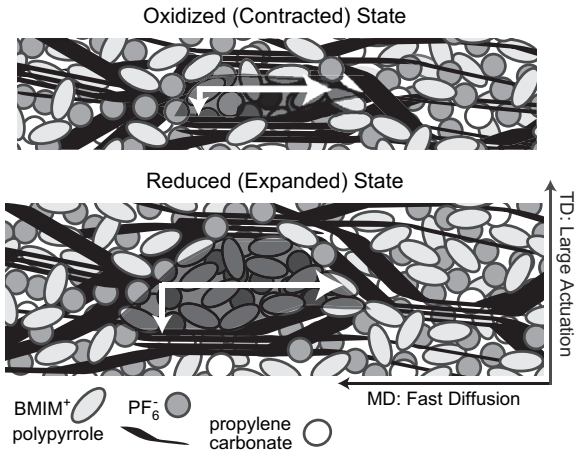

Fig. 14. Change in interchain spaces upon oriented polymer actuation in BMIMPF6. After warm-up, the interchain spaces are swollen with PF_6^-, propylene carbonate, and $BMIM^+$ cations. In oriented polypyrrole films, the chain axes and bundles preferentially align in the MD. This causes the spaces between chains to become elongated in the MD, providing a longer path of easy diffusion for small molecules in the MD than in the TD. A single interchain space is highlighted in grey, while its anisotropy is shown by the white arrows. Upon reduction in neat BMIMPF6, $BMIM^+$ cations swell the interchain spaces, pushing non-bundled chain segments apart. This causes a large actuation perpendicular to the chain axis. In processed films, the chain axes are oriented in the MD, so this large actuation is observed in the TD.

Even though we are interested in actuation in the MD and TD, one should note that the largest counterion influx and expulsion likely occurs along the ND (the direction with both the largest surface area and shortest diffusion distance). In the stretched (uniaxial) films, the diffusion rate in the ND and TD should be equivalent, but the diffusion length to the center of the film is 100× shorter in the ND than the TD. In the rolled case, forces applied to the films during the rolling process may cause the interchain and interbundle spaces to collapse in the film thickness (ND) direction, impeding the movement of counterions. We observe an increase in density when polypyrrole films are stretched or rolled, with a 2.3% increase for films stretched to a conductivity ratio of $(\sigma_{MD}/\sigma_{TD})_S = 3$, and a 2.7% increase for films rolled to $(\sigma_{MD}/\sigma_{TD})_R = 2.8$. The decreased electroactive performance of the rolled films when compared to the stretched films may be due to a more tightly packed microstructure resulting in lower counterion mobility in the ND.

5. Conclusions

We sought to improve polypyrrole actuators by attaining a better understanding of the microstructure of polypyrrole and manipulating this microstructure to improve electroactive properties. Based on X-ray diffraction and electrochemical experiments, a more detailed microstructural description consisting of disordered polypyrrole chains held together by small crystalline bundles, around which solvent and counterions are randomly distributed is proposed. Different processing techniques were utilized to achieve uniaxial and biaxial textures in polypyrrole films, and by processing the films such that the chain axes are preferentially oriented parallel to the MD, a much larger electroactive response is concentrated in the TD. This results in an actuator that shows a 100% increase in active strain when compared to as-deposited films actuated under the same electrochemical conditions, and electroactive strains of up to 11.3% have been achieved. Stretched films (with uniaxial orientation) exhibit superior electroactive properties to rolled films (with biaxial orientation), probably due to faster ion transport into the film along the ND.

Orientational processing of polypyrrole films provides a simple way to improve the performance of this electroactive material without altering the chemistry of deposition or actuation. The electrochemical properties of polypyrrole films remain unchanged after orientational processing, but the stress or strain that results from that electrochemistry is improved because it is concentrated in the direction of testing. By the addition of a processing step between deposition and actuation engineers can at least double the performance of their

polypyrrole-powered devices. Furthermore, these films provide anisotropic linear actuation not previously achievable in conducting polymers. This has exciting implications for electroactive device design, especially in applications such as biomimetic robotics, where complex bending motions are necessary to emulate fish or insect movement. An anisotropic polymer actuator could control the direction of actuation via its material properties, reducing the complexity of the mechanical transmission system needed.

Acknowledgement

This material is based on work supported by the U.S. Army Research Laboratory and the U.S. Army Research Office under Contract No. DAAD-19-02-0002. The authors would like to thank Professor Carl Michal and Jennifer Chien-Hsin Tso for valuable discussions, and recognize Dr. Nathan Vandesteeg for his work in developing the electrochemical dynamic mechanical analyzer used in this work.

References

[1] Smela E, Gadegaard N. Advanced Materials 1999;11(11):953.
[2] Naoi K, Oura Y, Maeda M, Nakamura S. Journal of the Electrochemical Society 1995;142(2):417–22.
[3] Hagiwara T, Hirasaka M, Sato K, Yamaura M. Synthetic Metals 1990;36:241–52.
[4] Yamaura M, Hagiwara T, Hirasaka M, Demura T, Iwata K. Synthetic Metals 1989;28(1–2):157–64.
[5] Yamaura M, Hagiwara T, Iwata K. Synthetic Metals 1988;20:209–24.
[6] Herod T, Schlenoff J. Chemistry of Materials 1993;5:951–5.
[7] Pytel R, Thomas E, Hunter I. Chemistry of Materials 2006;18(4):861–3.
[8] Hara S, Zama T, Takashima W, Kaneto K. Synthetic Metals 2005; 149(2–3):199–201.
[9] <ftp://dell.chem.sunysb.edu/pub/polar/>.
[10] Vandesteeg N. Synthesis and characterization of conducting polymer actuators. Ph.D. thesis. Department of Materials Science and Engineering, Massachusetts Institute of Technology; 2007.
[11] Nogami Y, Pouget JP, Ishiguro T. Synthetic Metals 1994;62:257–63.
[12] Osagawara M, Funahashi K, Demura T, Hagiwara T, Iwata K. Synthetic Metals 1986;14(1–2):61–9.
[13] Geiss RH, Street GB, Volksen W, Economy J. IBM Journal of Research and Development 1983;27(4):321–9.
[14] Wynne K, Street B. Macromolecules 1985;18:2361–8.
[15] Yoon CO, Sung HK, Kim JH, Barsoukov E, Kim JH, Lee H. Synthetic Metals 1999;99:201–12.
[16] Wernet W, Monkenbusch M, Wegner G. Makromolecular Chemistry Rapid Communications 1984;6:157–64.
[17] Blackwell J, Nagarajan MR. Polymer 1981;22(2):202–8.
[18] Briber R. Investigations of the structure and morphology of random block copolymers. Ph.D. thesis. Polymer Science and Engineering, University of Massachusetts; 1984.
[19] Bonart RJ, Morbitzer L, Hentze GJ. Journal of Macromolecular Science Part B: Physics 1969;3(2):337.
[20] Pouget JP, Oblakowski Z, Nogami Y, Albouy PA, Laridjani M, Oh EJ, et al. Synthetic Metals 1994;65:131–40.
[21] Kunugi T, Okuzaki H. Journal of Polymer Science Part B: Polymer Physics 1996;34:1269–75.
[22] Lesueur D, Alberola ND. Synthetic Metals 1997;88(2):133–8.
[23] Warren MR, Madden JD. Materials Research Society Symposium Proceedings 2005. 871E(I6.1).
[24] Warren MR, Madden JD. Synthetic Metals 2006;156(9–10):724–30.
[25] Ue M. Journal of the Electrochemical Society 1994;141(12):3336–42.
[26] Warren BF. X-ray diffraction. Reading, Massachusetts: Addison-Wesley; 1969.
[27] Kakudo M, Kasai N. X-ray diffraction by polymers. New York, NY: Elsevier Publishing Company; 1972.
[28] Lin X, Li J, Smela E, Yip S. International Journal of Quantum Chemistry 2005;102:980–5.
[29] Lu W, Fadeev AG, Qi BH, Smela E, Mattes BR, Ding J, et al. Science 2002;297(5583):983–7.
[30] Ding J, Zhou DZ, Spinks G, Wallace G, Forsyth S, Forsyth M, et al. Chemistry of Materials 2003;15(12):2392–8.
[31] Xia JL, Wang CH. Journal of Polymer Science Part B: Polymer Physics 1992;30(13):1437–42.
[32] Boersma A, Cangialosi D, Picken SJ. Polymer 2003;44(8):2463–71.